ORAL REFERENCE: ICF100671OR

THERMAL FAILURE OF THERMAL BARRIER CERAMIC COATING

Y. C. Zhou[1,2], T. Hashida[1]

[1]Fracture Research Institute, Tohoku University, Sendai, 980-8579, Japan
[2]Institute of Fundamental Mechanics and Material Engineering, Xiangtan University, Xiangtan, Hunan, 411105, China

ABSTRACT

The paper presents the experimental investigation on the fracture of thermal barrier ceramic coating (TBC) at high temperature. The fracture was induced by temperature gradient along TBC system thickness direction and oxidation between TBC and bond coat. Laser heating method was used to simulate the operating state of TBC system. Micro-observation and acoustic emission (AE) detect both revealed that fatigue crack was in two forms: surface crack and interface delamination. One can understand the failure mechanism from the plane of TBC surface temperature and substrate surface temperature. It was found that the life of thermal fatigue was reduced by the formation of alumina at interface. On the other hand, it was found that the temperature gradient between inner and outer surface of specimen accelerates the growth of alumina layer.

KEYWORDS

Thermal barrier ceramic coating, thermal fracture, temperature gradient, oxidation

INTRODUCTION

A thermal barrier ceramic coating (TBC) provides performance, efficiency, and durability benefits by reducing turbine cooling air requirements and lowering metal temperatures. The study of TBC is to develop a technology to protect alloy and make it to operate at 1500^0C and to realize 50% of thermal efficiency. Previous work has demonstrated that there are some important effects on TBC system operating life. The first effect is thermal fatigue [1,2]. High temperature heating and low or fast cooling must induce thermal stress loading and unloading for many cycles. The second effect is thermal growth oxidation (TGO) between bond coat and thermal barrier ceramic coating[3,4]. Generally, the composition of TGO is brittle ceramic, such as alumina (Al_2O_3). The cycles of high temperature loading and unloading not only make TGO to thicken but also make micro-voids and micro-cracks formation in TGO. On the other hand, the degradation of TGO may induce the spallation or delamination of thermal barrier ceramic coatings. The third is the surface roughness of bond coat[5,6]. The effect makes the formation of tensile stress at the peaks of interface undulation or compress stress at the valleys of interface undulation at cooling stage. The fourth is oxygen and sulfur penetration along grain boundaries[7]. Their effect causes the thermal barrier ceramic coatings to thin and consequence the function of TBC is weakened. However, in the real TBC system, the temperature gradient along TBC system thickness direction and TGO between bond coat and ceramic coating are the key factor of TBC system service life[8-10]. In this paper, the failure characteristics of TBC at high temperature induced by temperature gradient and TGO were investigated.

MATETIALS AND EXPERIMENTAL METHOD

Heating Method

In order to study the above-mentioned effects, one needs to design an experimental method to simulate the operating state which has the temperature gradient in the TBC system thickness direction, many cycles of heating/cooling. The simulating system was laser heat method in which heating of specimen surface was accomplished using a continuous CO_2 laser of 10.6μm output wavelength. The unit was nominally specified as a 50W laser. The system was arranged so that the coated specimens could be exposed to a laser beam with a preset size (such as 8mm or 6mm in diameter), duration and intensity. The specimen was internally gas-cooled to achieve various temperature drops within the coating layer. The computer-controlled system shown in Figure 1 allowed heating/cooling processes to be automatically cycled.

The temperatures on ceramic coating surface and on substrate surface were monitored by means of a general infrared radiation pyrometer and thermocouple, respectively. Concurrently with the heating tests, acoustic emission (AE) monitoring was performed to detect the micro-fracture process of the coating materials. The disposition of the two or three transducers enabled the determination of the linear location of the AE sources emitted from the sample. Furthermore, AE signal analysis can be used to provide a way to predict the long term behavior of the TBC under thermal-cycling conditions. AE signals were detected using a broad band piezoelectric transducer with a resonant frequency close to 1MHz. The square of signal peak voltage was used as a measure of AE energy. Impedance spectroscopy (IS) was used to evaluate the formation kinetics and physical properties of the reaction layer between bond coat and ceramic coating. In the evaluations of TBCs degradation, the IS method was developed to detect various defects such as delamination, spallation and cracks and other damages.

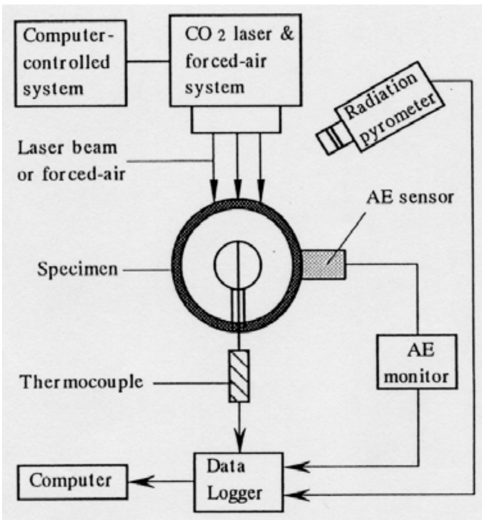

Figure 1: Schematic of the experimental setup for CO_2 laser heating method

Materials and Specimens

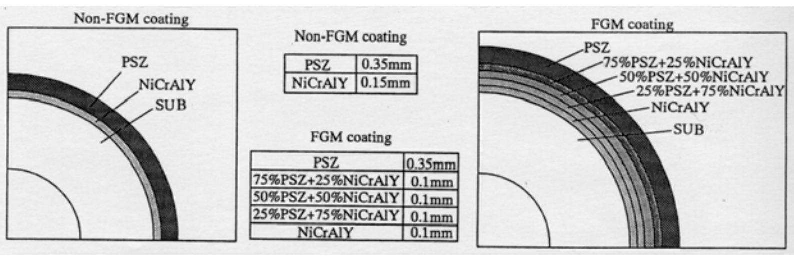

Figure 2: Schematics of the cross-sections of two types of coatings.

Two types of materials samples were prepared. One was conventional coating (non-FGM) which was a two-layer coating system consisting of PSZ layer (partially stabilized ZrO_2 by 8 wt%Y_2O_3) over a NiCrAlY bond coat. The coatings were air-plasma-sprayed onto a substrate. The material of the substrate was cylindrical Ni base superalloy which simulated radius of leading edge for gas turbine blade. Recently, multi-layer coating system, in particular, the functionally graded material (FGM) coating system has been proposed. The FGM coating was a five-layer coating system of PSZ and NiCrAlY, and the composition was designed to have the same thermal shielding performance as that of the non-FGM coating. Figure 2 shows the schematics of the cross-sections of non-FGM and FGM coatings.

EXPERIMENTAL RESULTS AND DISCUSSIONS

Crack characteristics

SEM (scanning electron microscope) observations indicated that laser heating produced two types of coating damage: vertical (or surface) cracking and interface delamination both in non-FGM and FGM coatings. The vertical cracking and interface delamination for non-FGM and FGM coatings exposed to laser heating are shown in Figure 3. SEM examination of the specimens' cross-sections showed that the delamination cracks in non-FGM coating always occurred just above the interface between bond coat NiCrAlY layer and PSZ layer. On the other hand, one can see that the interface crack kinks out the main crack as shown in the figure. However, the delamination cracks in FGM coating always occurred close to two interfaces: the interface between PSZ layer and 75%PSZ/25%NiCrAlY layer, and between 75%PSZ/25%NiCrAlY layer and 50%PSZ/50NiCrAlY layer. The final complete failure was spallation due to the interface delamination growth.

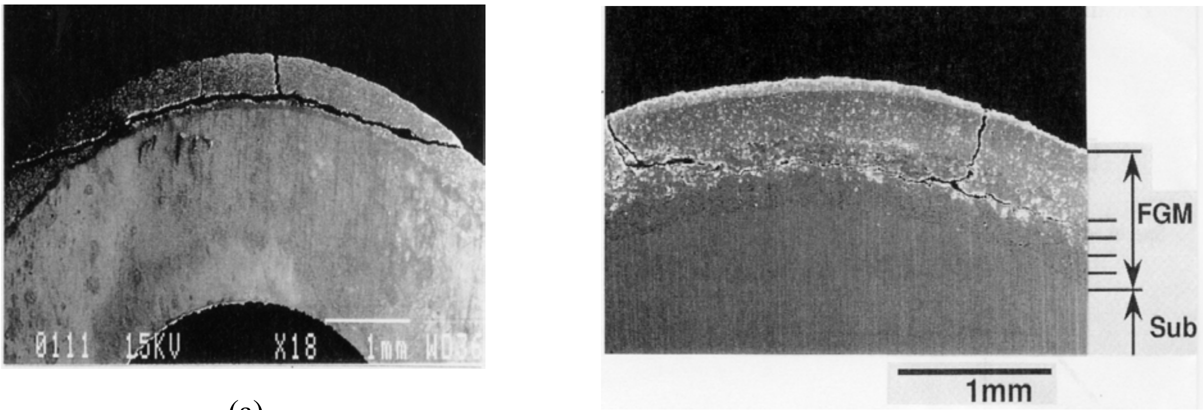

(a) (b)

Figure 3. SEM micrographs showing vertical cracking and interface delamination cracking: (a) non-FGM coating subjected to 6 thermal fatigue cycles, where the exposed time for every cycle was 70s and the highest temperature on coating and substrate was 1200^0C and 600^0C, respectively. (b) FGM coating subjected to 10 thermal fatigue cycles, where laser power was 34W.

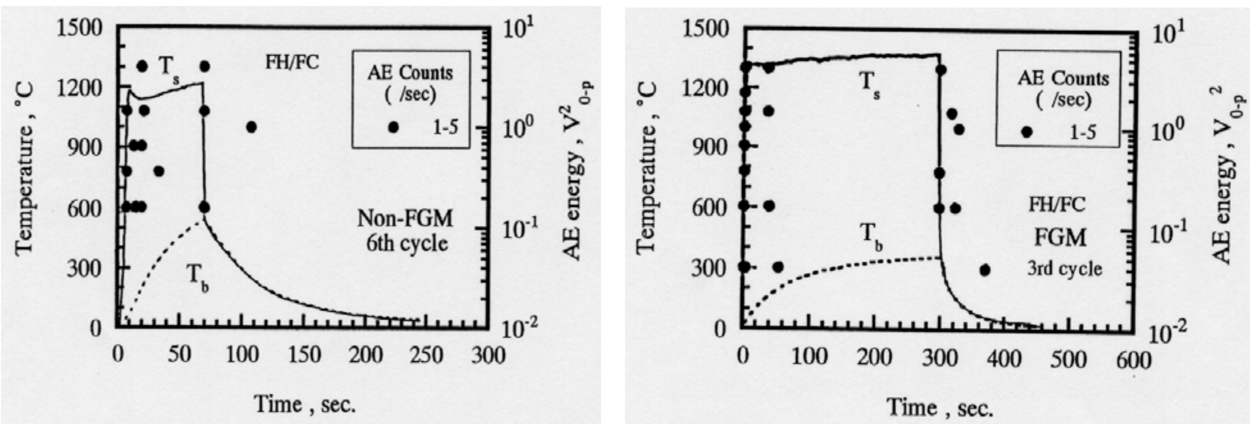

(a) (b)

Figure 4: Temperature histories and AE activity in non-FGM and FGM coating during laser heating: (a) non-FGM coating subjected to 6 thermal fatigue cycles, where the exposed time for every cycle was 70s and the highest temperature on coating and substrate was 1200^0C and 600^0C, respectively. (b) FGM coating subjected to 3 thermal fatigue cycles.

Temperature histories and AE monitoring results in the laser thermal fatigue tests were also obtained as shown in Figure 4. It was found that AE signals were recorded most often in the periods of heating or cooling. AE signals were recorded even on the later stage of cooling, i.e., the temperature gradient was zero. The comparison of AE behavior and SEM observation indicated that first AE signal detected corresponds to the vertical cracking. The high energy of AE signals after the first AE signal recorded was associated with interface delamination cracking growth. This means that vertical (or surface) crack can more easily take place than interface delamination cracking. On the other hand, no delamination growth was observed for FGM coating within the tested temperature range where non-FGM coating showed extensive delamination.

Fracture mechanism map

One finds that temperature drop through specimen thickness is an important parameter to analyze failure mechanism such as vertical crack and interface delamination crack. The observed damage modes correlated with temperature conditions, T_s-T_b are shown in Figure 5, where T_s and T_b are, respectively the temperature on the surface of coating and substrate. In the figures, the temperature is maximum values recorded during a heating-cooling cycle. Experimental data for uniform heating are also included, which were obtained from furnace heating-cooling tests. It is convenient to use the T_s-T_b plane to study the failure threshold of TBC system. The physical concept is also clear and the optimum state for temperature range of advanced gas turbine can also be obtained on the T_s-T_b plane. In the plane, one can distinguish three regions which are no crack region, vertical crack region and delamination region. From the T_s-T_b plane, one can have the conclusion that FGM coating has much higher thermal fatigue resistance compared to non-FGM coating system through thermal cycling tests conducted under the simulated advanced gas turbine blade conditions.

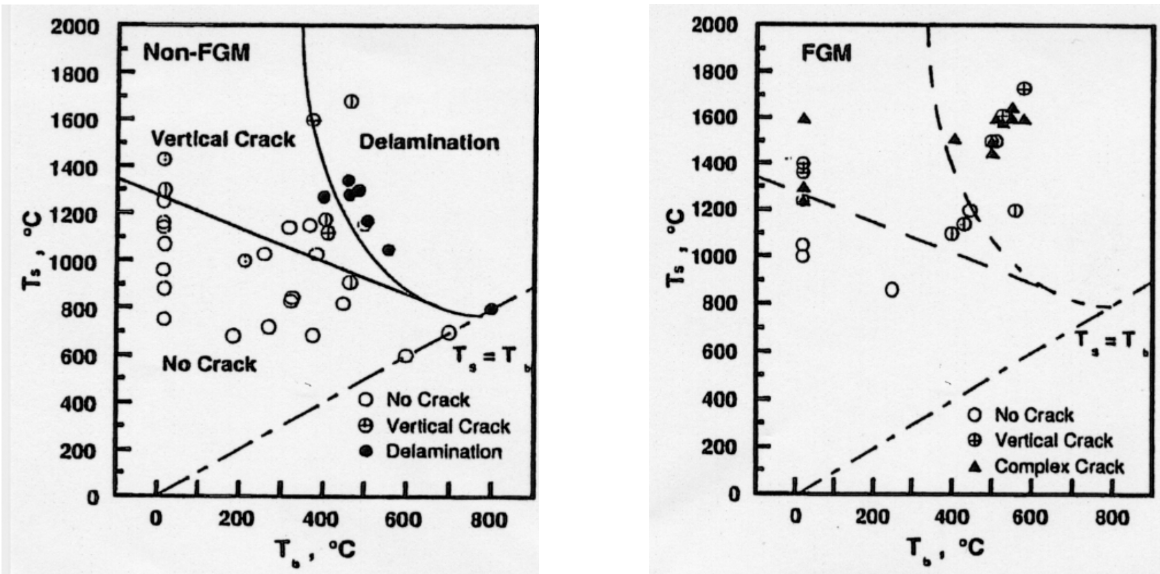

(a) (b)

Figure 5: Fracture mechanism map in the T_s-T_b plane, (a) non-FGM coating, (b) FGM coating.

Interface crack

From the AE characteristics of coating failure process it is possible to correlate the sum of AE energy recorded during heating and cooling process with the total length of delamination crack. The correlation is shown in Figure 6(a) and (b) for non-FGM coating and FGM coating, respectively. The total length of the delamination cracks for FGM coating shown in Figure 6(b) is the sum of the length of the delamination cracks at two interfaces as described in the above. It is seen that there is a general correspondence between AE energy and delamination length for two coating systems. For non-FGM coating, the correlation is approximately linear, although considerable experimental scatter is observed. In contrast, the correlation is nonlinear for FGM coating. The data both in Figure 6(a) and (b) are different from each other in different heating or cooling rate and cycle number.

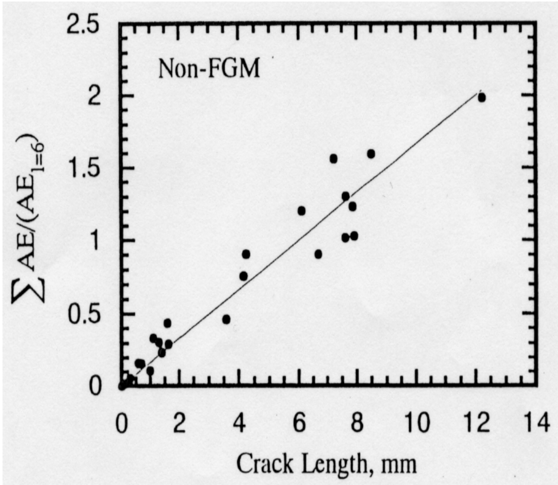

(a) Non-FGM

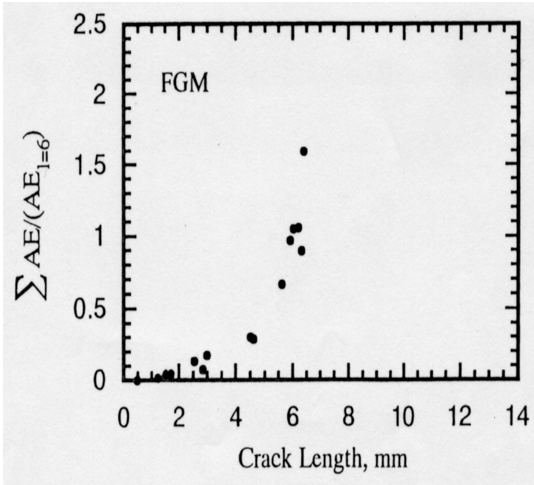

(b) FGM

Figure 6: Total energy of AE versus total length of delamination, (a) non-FGM coating, (b) FGM coating.

Influence of oxidation on the thermal fatigue failure

In order to understand the effect of TGO on the thermal fatigue properties, thermal fatigue tests were performed heat cycle of simulated real plant with as-received and pre-aged non-FGM specimen. The pre-aged specimen was heated by furnace for 4000 hours at 1000^0C. In this case, the formation of 12µM thickness oxide was observed at the interface between TBC and NiCrAlY bond coating.

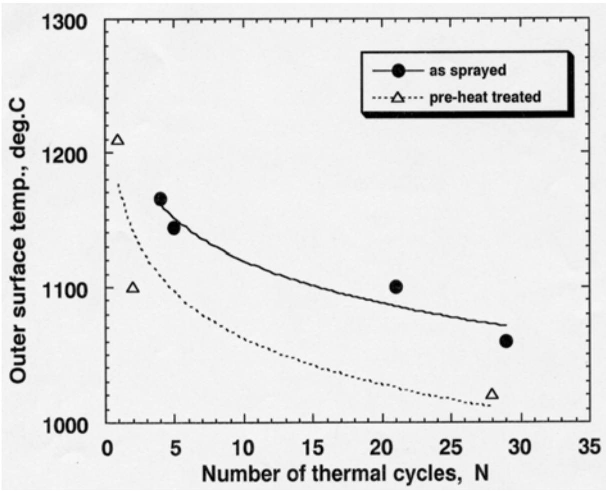

Figure 7: Relationship between surface temperature and fracture cycles of thermal fatigue test.

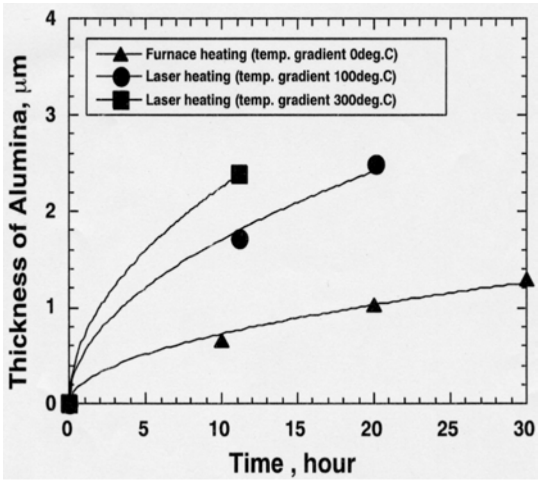

Figure 8: Comparison between furnace and laser heating concerning time dependence of alumina thickness

The relationship between surface temperature and thermal cycle of failure is shown in figure 7. Failure cycle increased accompanied with surface temperature decreased both in received and pre-aged specimen. However, in case of equality in the surface temperature of both, pre-aged specimen was earlier degradation than non-aged specimen. Moreover, almost all cracks formed at interface between top coating YSZ and oxide. These cracks are confirmed by SEM observation. This means that the oxide is bad influence in terms of thermal fatigue properties. Furthermore, the oxide is identified as Al_2O_3 (alumina) by energy dispersive x-ray spectroscopy (EDX). Thermal stress can be induced by the formation of alumina. Consequently, evaluation of oxidation behavior, especially alumina formation and growth, is very important for understanding of coating degradation.

Influence of temperature gradient on oxidation

In order to understand the effect of temperature gradient on the oxide growth, the alumina thickness was measured for the non-FGM specimen heated by CO_2 laser heating or furnace heating. In the former case, there was a temperature gradient along TBC system thickness direction. Moreover, the temperatures were not only measured on surface and backside but also at interface between YSZ and MCrAlY by thermo-couples. The temperature on backside surface was kept on 800^0C or 600^0C and the temperature at interface was kept on 900^0C. This means that the temperature gradients were 100^0C and 300^0C, respectively. In the later case, there was zero temperature gradient along TBC system thickness direction. In the furnace heating, the temperature was kept 900^0C. The relationship between alumina thickness and aging time was obtained. The result is represented in Figure 8 with result of the uniform heated as for same aging temperature. As the result, in spite of equal YSZ/NiCrAlY interface temperature between the non-uniform heated specimen and uniform heated one, the alumina thickness are markedly different. The alumina is thicker for non-uniform heated case than that for uniform heated case. Namely, smaller temperature gradient forms thicker alumina than large gradient. The reason of the phenomenon is that the diffusion of oxygen through the YSZ accelerates in order to being high temperature concerning YSZ surface in case of laser heating as local heat. Moreover, due to the laser heated specimen has many porosity accompanied by formation of microcracks by virtue of larger thermal stress, oxygen rapidly penetrates interface through microcracks. Accordingly, laser heating which has temperature gradient is more effective condition in order to evaluation of oxidation behavior of real plants.

CONCLUSIONS

The thermal fracture in thermal barrier ceramic coating system was experimentally investigated. The fracture was induced by temperature gradient along TBC system thickness direction and oxidation between TBC and bond coat. Laser heating method was used to simulate the operating state of TBC system. The obtained results are arranged as follows.

(1) The failure of TBC system was in two crack forms: surface crack and interface delamination. The final complete failure was spallation due to the interface delamination growth.

(2) A fracture mechanism map in the T_s-T_b plane was obtained, where T_s and T_b are, respectively the temperature on the surface of coating and substrate. One can understand the effect of temperature gradient on TBC system service life.

(3) The life of thermal fatigue was reduced by the formation of alumina at interface. To sum up, the alumina has a bad influence on thermal fatigue property due to existence of thermal stress.

(4) The temperature gradient between inner and outer surface of specimen accelerates the growth of alumina layer.

ACKNOWLEDGMENTS

The collaborative research for foreign researchers in Japan is provided to first author YCZ by JSPS (Japan Society for the Promotion of Science). This support is gratefully acknowledged. A part of this work was supported by the Grant-in-Aid for COE (Center of Excellence) Research (No. 11CE2003), The Ministry of Education, Science, Sports and Culture. The authors express their appreciation to the grant.

REFERENCES

1. Takeuchi, Y. R. and Kokini, K. (1994) *Trans. ASME, J. Engng Gas Turbines Power*, 116, 266.
2. Zhu, D. M. and Miller, R. A. (1998) *Mater. Sci. Engng. A*, 245, 212.
3. Cheng, J., Jordan, E. H., Barber, B. and Gell, M. (1998) *Acta Mater.*, 46, 5839.
4. Tolpygo, V. K., Dryden, J. R. and Clarke, D. R. (1998) *Acta Mater.*, 46, 927.
5. He, M. Y., Evans, A. G. and Hutchinson, J. W. (1998) *Mater. Sci. Engng. A*, 245, 168.
6. Wang, J. S. and Evans, A. G. (1999) *Acta Mater.*, 47, 699.
7. Bernstein, H. L., Allen, J. M. (1992) *J. Engng Gas Turbines Power*, 114, 293.
8. Zhou, Y. C., Hashida, T. (2001) *Int. J. Solids Structures*, 38, 4235.
9. Zhou, Y. C. and Hashida, T. (2001) *Int. J. Fatigue*, (in press)
10. Zhou, Y. C., Hashida, T. (2001) *Trans. ASME J. Engng Gas Turbines Power*, 23, (in press)